ISBN: 978-3-95450-232-5 ISSN: 2673-7000 doi:10.18429/JACoW-NAPAC2022-WEPA85

LOCALIZED BEAM INDUCED HEATING ANALYSIS OF THE EIC VACUUM CHAMBER COMPONENTS*

M. Sangroula†, J. Bellon, A. Blednykh, D. Gassner, C. Hetzel,
C. Liaw, C. Liu, P. Thieberger, S. Verdu-Andres
Brookhaven National Laboratory, Upton, NY 11973, USA

Abstract

The Electron-Ion Collider (EIC), to be built at Brookhaven National Laboratory (BNL), is designed to provide a high electron-proton luminosity of $10^{34}\,\mathrm{cm}^{-2}\,\mathrm{sec}^{-1}$. One of the challenging tasks for the Electron Storage Ring (ESR) is to operate at an average beam current of 2.5 A within 1160 bunches with a ~ 7 mm rms bunch length. The Hadron Storage Ring (HSR) will accumulate an average current of 0.69 A within 290 bunches with a 60 mm rms bunch length for the worst-case scenario in terms of thermal heating, although it will have 1 A with 1160 bunches for the high luminosity. Both rings require impedance budget simulations. The intense e-beam in the ESR can lead to the overheating of vacuum chamber components due to localized metallic losses and synchrotron radiation. This paper focuses on the beam-induced heating analysis of the ESR vacuum components including BPM, standard RF shielded bellows, and gate valve. To perform thermal analysis, the resistive loss on individual components is calculated with CST and then fed to ANSYS to determine the temperature distribution on the vacuum components. Preliminary results suggest that active water cooling will be required for most of the ESR vacuum components. Similar approach is applied for the HSR vacuum components. The thermal analysis of the HSR stripline injection kicker is presented.

INTRODUCTION

The intense beams of the ESR and HSR produce a large amount of beam-induced resistive losses that can lead to the overheating of EIC [1–3] vacuum chamber components. The impedance analysis of both the ESR and HSR vacuum chamber components can be found in [4–6]. In this paper, we present the thermal analysis of those components. To perform thermal analysis, the resistive loss on individual components is calculated using the 3D electromagnetic code CST [7], whose result is fed into the another code ANSYS [8] to determine the temperature distribution.

ESR COMPONENTS

Most of the ESR vacuum chamber components have elliptical profile having 80 mm horizontal, and 36 mm vertical dimension. These components experience maximum local heating with an average beam current of 2.5 A (27.6 nC per bunch) from 1160 bunches that are only 7 mm long. Therefore, we used these beam parameters to calculate the local metallic losses for all the ESR components. We present our thermal analysis due to a central beam (no lateral offset) for the BPM, standard RF shielded bellows, and gate valve, which we discuss in the following subsections. In some regions of the ESR, beam experiences slight lateral offset for which the corresponding thermal analysis need to be done.

Beam Position Monitor (BPM)

The ESR BPM button design is shown in Fig. 1, that consists of total four molybdenum buttons (two on top and two on bottom). It has an elliptical shaped copper beam chamber having water cooling channels on the both sides of the horizontal plane. We chopped the beam chamber longitudinally into six small sections to calculate corresponding metallic losses to perform more accurate thermal analysis.

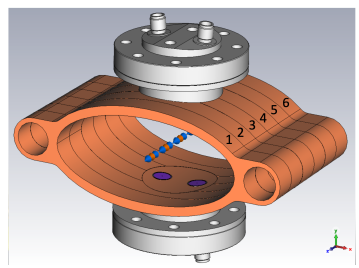

Figure 1: ESR BPM button design.

Figure 2(a) depicts a cut view of the BPM showing the internal design of the feedthroughs, and BPM buttons. The BPM buttons have a diameter of 7 mm, and the gap between the BPM housing and the button is 250 µm. We used CST Wakefield Solver with the ESR beam parameters (I_{avg} = 2.5 A, M = 1160, σ = 7 mm) to calculate the resistive wall loss for this BPM which are listed in Table 1.

Table 1: Metallic Loss on the ESR BPM

Components	Material	Loss (Watts)
4-buttons	Mo	0.288
4-stems	Mo	0.017
4-pins	Cu	0.003
4-connectors	St. St. 316L	0.015
4-cavity liners	St. St. 316L	0.998
2-flanges	St. St. 316L	0.348
2-gaskets	Cu	0.198
2-surface sheets	Cu	1.033
Housing	St. St. 316L	2.231
Beam chamber	Cu	3.983
Total	**NA**	**9.114**

* Work supported by Brookhaven Science Associates, LLC under Contract No. DE-SC0012704 with the U.S. Department of Energy.
† msangroul@bnl.gov

ISBN: 978-3-95450-232-5 ISSN: 2673-7000 doi:10.18429/JACoW-NAPAC2022-WEPA85

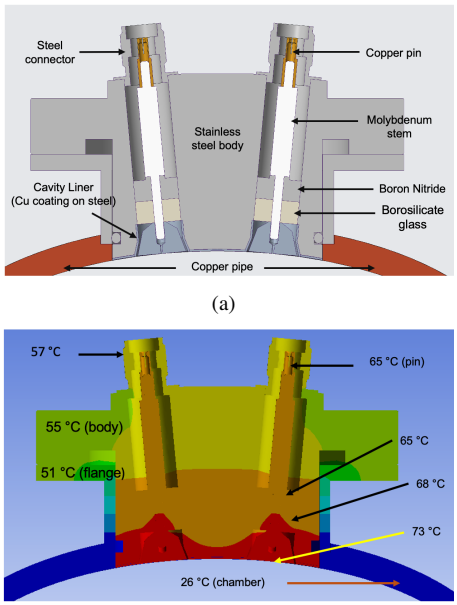

Figure 2: ESR BPM section showing the (a) internal structure of the buttons and (b) thermal distribution.

The individual losses, listed in Table 1, are fed into the another code ANSYS along with a heat sink that flows water at 25°C via cooling channels at the rate of 6 gallons per minute, to find the thermal distribution. The simulated temperature distribution is shown in Fig. 2(b), which shows that the maximum temperature is 73°C at the BPM button surface. Although this temperature seems manageable, we are exploring other options for further reduction.

Standard RF Shielded Bellows and Gate Valve

The ESR standard RF shielded bellows and gate valve also have the same elliptical profiles as that of the ESR BPM. Figure 3(a) shows a simplified design of this standard bellows containing flexible RF-fingers which reside on the RF-sleeve externally to maintain a good RF-contact. The overlap between the RF-sleeve and fingers creates a local cavity of 0.5 mm depth. Both the RF-sleeve and the fingers are attached to the inner flanges at their ends. The outer flanges are made out of CuCrZr, while the inner flanges are made from stainless steel 304L. The RF-sleeve has 10-microns sliver plated on top of stainless steel 304L.

The ESR gate valve design, Fig. 3(b), is also similar to that of the standard bellows in the sense that it has a local cavity of 1 mm depth at the middle of the RF-bridge containing longitudinal slots. Though the actual design has longitudinal slots on the RF-bridge, made out of 10-microns sliver plated stainless steel, the simulation geometry does not contain those slots. In addition, the outer flanges and inner flanges are mostly similar to that of the ESR bellows design and are made out of the same materials; CuCrZr, and stainless steel 304L respectively. A copper gasket is placed between the inner and outer flanges for both of these designs, which in

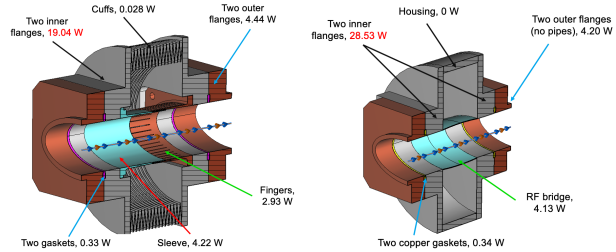

Figure 3: Simplified CAD models for the ESR (a) standard RF shielded bellows and (b) gate valve.

the real machine will be in between the joints of bellows and gate valve.

Again, we ran CST simulation using the ESR beam parameters for the both ESR bellows and gate valve, and the corresponding metallic losses for individual components are evaluated, which are stated in the same Fig. 3. Using these values of metallic losses, we have calculated the thermal distribution for a more realistic structure rather than individual geometry, which we discuss this in the following subsection.

Thermal analysis for a more realistic model In the real machine, both the bellows and gate valve are sandwiched between dipole and multipole chambers of the ESR as shown in Fig. 4(a). A relativistic electron beam emits synchrotron radiation tangentially while passing via a bending magnet. This radiation hits outer wall of these dipole and multipole chambers and leads to increase in temperature. To alleviate this issue, water cooling channels are placed on both side of these chambers. The power loss due to synchrotron radiation are calculated (outboard side only) using the code SynRad, which are found to be 500 W and 2750 W for the dipole and multipole chambers respectively. In addition, the resistive losses on the dipole and multipole chamber are found to be 16 W and 64 W, respectively.

Thermal simulation was performed for the entire geometry shown in Fig. 4(a) using the ANSYS code by considering both the resistive wall and the synchrotron radiation losses, and circulating water via cooling channels at the rate of 6 gallon per minute at 38°C (average). Here we assumed elevated water temperature as it had already absorbed some heat from the upstream components. Initial simulation showed the maximum temperature of 142°C at the ESR bellows sleeve, Fig. 4(b). Therefore, to reduce this high temperature, we added water cooling channels, as shown in the Fig. 4(c), to each of the bellows' flanges. We circulated water at the rate of 1 gallon per minute at 25°C and re-run the ANSYS simulation. In this case, we were able to reduce the maximum temperature from 142°C to 95°C as shown in Fig. 4(d). In addition, the location of maximum temperature is found at the outboard side of the dipole chamber, which is due to the synchrotron radiation.

ISBN: 978-3-95450-232-5 ISSN: 2673-7000 doi:10.18429/JACoW-NAPAC2022-WEPA85

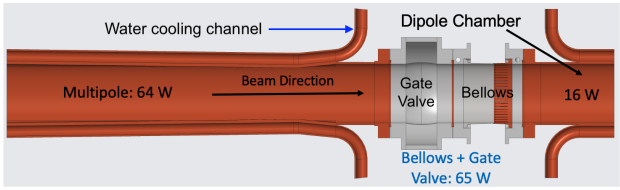

(a)

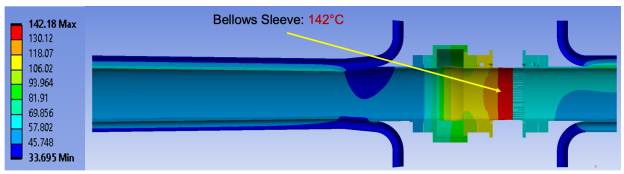

(b)

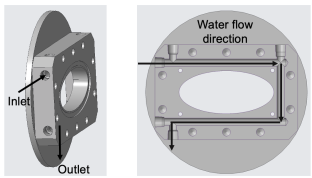

(c)

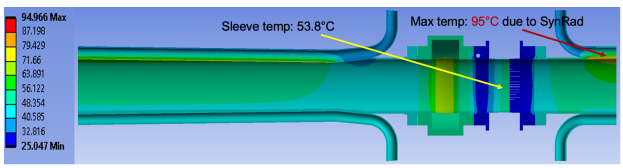

(d)

Figure 4: (a) More realistic geometry of the ESR vacuum chamber containing RF shielded bellows and gate valve between dipole and multipole chambers, (b) thermal distribution corresponds to geometry (a), (c) bellows' flange displaying the water cooling channel, and (d) thermal distribution with the added water cooling in each bellows' flange.

HSR COMPONENTS

The EIC Hadron Storage Ring (HSR) will accumulate an average current of 0.69 A from 290 bunches with a 60 mm rms bunch length for the worst case scenario in terms of resistive wall heating, although it will have 1 A with 1160 bunches for the high luminosity. We plan to evaluate the beam induced heating for all the HSR vacuum chamber components including collimator, bellows, and others. Here, we focus on the thermal simulation of the stripline injection kicker.

The basic design parameters for the HSR injection kicker including its initial geometry can be found in Ref. [9], and its latest design update can be found in Ref. [10]. Figure 5 shows the latest geometry of this kicker, which is about a meter long structure having two curved electrodes separated by 59 mm. Two dielectric (alumina) supports on each electrode helps to prevent the electrode from deformation due to beam induced heating. In addition, four venting ports are placed to maintain a good vacuum inside the kicker.

We calculated the individual metallic losses for the HSR stripline injection kicker with the 60 mm rms bunch length

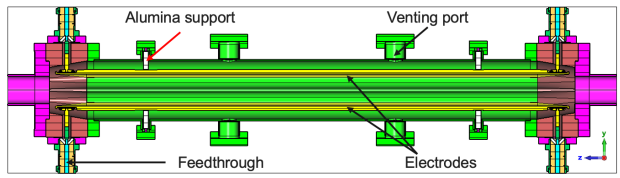

(a)

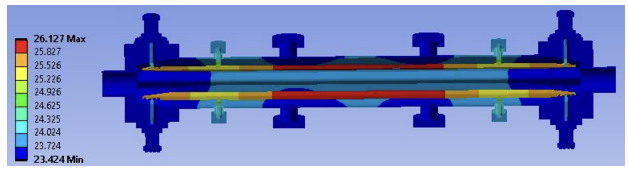

(b)

Figure 5: (a) Cut view of the HSR injection kicker geometry, and (b) corresponding thermal distribution.

using CST, which are listed in Table 2. For this simulation, we used 25-microns copper plated stainless steel material. In reality, we plan to coat a thin layer (~nano-meter) of amorphous carbon on top of copper coating to reduce Secondary Electron Yield (SEY).

Table 2: Metallic Loss on HSR Injection Kicker

Components	Loss (Watts)
Housing with 2-inner flanges	0.78
2-electrodes	0.58
4-feedthroughs outer cylinder (Nickel)	0.68
4-feedthroughs inner pin (Nickel)	0.95
2-end-cavities holding feedthrough	0.19
4-kovar pins and screws	0.25
2-outer flanges with beam pipe	0.19
Others (venting ports, wire mesh)	0.07
Total	**3.69**

The thermal distribution obtained from ANSYS simulation for this injection kicker using the value of resistive losses listed in Table 2 is depicted in Fig. 5(b), which shows that the maximum temperature is ~ 26°C, assuming the room temperature of 22°C.

SUMMARY AND FUTURE WORKS

In this paper, we presented our beam induced heating analysis for the several EIC vacuum chamber components. Preliminary results indicates the requirement of active water cooling for the most of ESR components. Future works will be focus on the analysis for the other vacuum chamber components, and for beam with lateral offset.

REFERENCES

[1] Electron-Ion Collider. https://www.bnl.gov/eic/

[2] C. Montag, E. C. Aschenauer, *et al.*, "Design Status Update of the Electron-Ion Collider," in *Proc. IPAC'21*, Campinas, Brazil, May 2021, pp. 2585–2588. doi:10.18429/JACoW-IPAC2021-WEPAB005

ISBN: 978-3-95450-232-5 ISSN: 2673-7000 doi:10.18429/JACoW-NAPAC2022-WEPA85

[3] F. Willeke and J. Beebe-Wang, "Electron Ion Collider Conceptual Design Report," 2021. doi:10.2172/1765663

[4] A. Blednykh *et al.*, "An Overview of the Collective Effects and Impedance Calculation for the EIC," in *Proc. IPAC'21*, Campinas, Brazil, May 2021, pp. 4266–4269. doi:10.18429/JACoW-IPAC2021-THPAB238

[5] G. Wang, M. Blaskiewicz, A. Blednykh, and M. P. Sangroula, "Studies of the Short-Range Wakefields for the Electron Storage Ring in the Electron Ion Collider," in *Proc. IPAC'21*, Campinas, Brazil, May 2021, pp. 2675–2678. doi:10.18429/JACoW-IPAC2021-WEPAB032

[6] A. Blednykh *et al.*, "Impedance Optimization of the EIC Interaction Region Vacuum Chamber," in *Proc. IPAC'21*, Campinas, Brazil, May 2021, pp. 4270–4273. doi:10.18429/JACoW-IPAC2021-THPAB239

[7] CST Studio Suite. https://www.3ds.com/products-services/simulia/products/cst-studio-suite/solvers/

[8] ANSYS Software. https://www.ansys.com/

[9] M. P. Sangroula *et al.*, "Optimization of the Hadron Ring Stripline Injection Kicker for the EIC," in *Proc. IPAC'21*, Campinas, Brazil, May 2021, pp. 3073–3076. doi:10.18429/JACoW-IPAC2021-WEPAB193

[10] M. P. Sangroula *et al.*, "Design Update on the HSR Injection Kicker for the EIC," in *Proc. IPAC'22*, Bangkok, Thailand, 2022, pp. 1904–1907. doi:10.18429/JACoW-IPAC2022-WEPOPT028